


## Article

# Research on the Reconstruction Method of Old Houses in Mindong, Republic of China, Based on a Wearable Mobile Scanning System

Jiayong Yu <sup>1</sup>, Xuejing Jiang <sup>1</sup>, Fei Xu <sup>2</sup>, Honggen Chen <sup>3</sup>, Wei Wu <sup>4</sup>, Ronghai Qiu <sup>2,\*</sup>, Wei Ma <sup>1</sup>, Yuanjie Liu <sup>3</sup> and Guoqiang Wu <sup>1</sup>

<sup>1</sup> College of Civil Engineering, Anhui Jianzhu University, Hefei 230601, China; yujiayongskd@163.com (J.Y.); jiangxuejing2022@163.com (X.J.); mawei@ahjzu.edu.cn (W.M.); wuguoqiang0909@163.com (G.W.)

<sup>2</sup> Institute of Urban Construction, Anhui Xinhua College, Hefei 230088, China; xufei\_sdkj@163.com

<sup>3</sup> 2nd Construction Co., Ltd. of China Construction 5th Engineering Bureau, Hefei 230051, China; hokence@163.com (H.C.); liuyuanjie133@163.com (Y.L.)

<sup>4</sup> Ningbo Institute of Surveying, Mapping and Remote Sensing, Ningbo 315042, China; nbgis@vip.163.com

\* Correspondence: qioronghai@axhu.edu.cn; Tel.: +86-17356311276

**Abstract:** To address the complex structures of historical buildings in Mindong, lack of historical reference materials, and heavy workload of traditional surveying and mapping methods in the field, a 3D reconstruction method of historical building based on a wearable mobile scanning system for data acquisition was studied. First, a wearable mobile scanning system is used to scan historical buildings in three dimensions. The data are fused to obtain high-precision three-dimensional point cloud data of historical buildings. Second, based on the processed point cloud, a 2D map of historical buildings is accurately drawn using point cloud slicing. Finally, three-dimensional reconstruction of historical buildings is realized using a 2D atlas of historical buildings and modern modeling technology. The accuracy of the three-dimensional reconstruction model was analyzed using a fitting algorithm and structural geometric relationship to verify the effectiveness and accuracy of the method. An old house in Mindong, Republic of China, was taken as the research object. Experimental analysis revealed that (1) a wearable mobile scanning system is suitable for high-quality point cloud data acquisition of buildings with complex geometric features, solving the problems of low efficiency and poor coverage of traditional surveying and mapping results; and (2) the method realizes 2D results rendering and 3D reconstruction of historical buildings based on the wearable mobile scanning system data with good accuracy, providing a reference for the protection and repair of historical buildings and health assessment.

**Keywords:** wearable mobile scanning system; digitalization of historical building; flat vertical section drawing; HBIM reconstruction; precision validation



**Citation:** Yu, J.; Jiang, X.; Xu, F.; Chen, H.; Wu, W.; Qiu, R.; Ma, W.; Liu, Y.; Wu, G. Research on the Reconstruction Method of Old Houses in Mindong, Republic of China, Based on a Wearable Mobile Scanning System. *Buildings* **2024**, *14*, 1766. <https://doi.org/10.3390/buildings14061766>

Academic Editors: Ehsan Noroozinejad Farsangi and Elena Lucchi

Received: 7 April 2024

Revised: 5 June 2024

Accepted: 6 June 2024

Published: 12 June 2024



**Copyright:** © 2024 by the authors. Licensee MDPI, Basel, Switzerland. This article is an open access article distributed under the terms and conditions of the Creative Commons Attribution (CC BY) license (<https://creativecommons.org/licenses/by/4.0/>).

## 1. Introduction

In this era of globalization, cultural heritage has become an important part of promoting national culture and ethnic diversity [1]. As an integral part of architectural heritage, historical buildings highlight the core values of national culture and ethnic diversity in history, culture, art, and science [2]. They are not only the “material witnesses of civilization” but also the value bearing of human behavior and ideological memory [3]. The natural and cultural conditions in the eastern Fujian region of China are complex and diverse [4]. Its traditional dwellings are an important branch of local historical architectural culture. They not only maintain the common characteristics of traditional Chinese residential buildings, such as a central axis symmetry, a courtyard connection, and wooden load-bearing systems, but also feature measures adjusted to local conditions and materials to form their own unique style with the humanistic characteristics of the “Minhai system”. However, with the

changes in times, some traditional dwellings in eastern Fujian have been affected by human activities and natural disasters. The reconstruction and expansion in recent years have led to different degrees of changes in their original style and structural characteristics, and there is a certain degree of damage. In addition, it is difficult for current homogeneous and modular architectural design to meet the demands of inheriting traditional architectural culture [5]. The details and accuracy of basic data largely restrict the effects of traditional building protection, appearance restoration, and three-dimensional (3D) reconstruction [6]. Therefore, complete basic data are essential for mastering architectural changes and building repairs and inheriting the architectural culture of traditional residential buildings in eastern Fujian. Traditional basic data acquisition methods are mostly derived from manual measurements or archived two-dimensional (2D) drawings made by technicians. However, the traditional methods are time consuming and have limitations [7]. Typical problems encountered in recording and repairing traditional buildings, such as the loss, damage, and low accuracy of paper documents, and the lack or change in building geometric information, make it necessary to use digital technology to reconstruct a 3D model with intuitive, extensible, and easy-to-interpret features to record traditional building information.

In the digital study of traditional residential buildings in eastern Fujian, the complete collection of point cloud data is important for realizing 3D reconstruction, protection, restoration, and research. Point cloud data acquisition technology includes 3D laser scanning, unmanned aerial vehicle (UAV) photogrammetry, red–green–blue depth cameras, and close-range photogrammetry [8]. Terrestrial laser scanning and UAV photogrammetry are the most widely used technologies and have achieved good data acquisition results and visual effects [9–11]. Terrestrial laser scanning technology can be used for orthophotos, 2D rendering, and 3D modeling. It has a high measurement accuracy for objects with irregular geometric shapes [12,13]. However, terrestrial laser scanning technology cannot be used to scan data in some complex areas. There are problems such as low efficiency and difficulty in achieving 100% coverage [14]. UAV photogrammetry technology can collect texture and environmental information of historical buildings through aerial photographs and videos to obtain more accurate data, and it has the advantages of high timeliness, flexibility, and spatial resolution [15]. However, owing to the processing and calibration accuracy of drone cameras, more distortion errors are generated when modeling complex structures [16]. Moreover, UAVs are mostly used to collect the appearance feature data of the target building; internal data cannot be collected. Compared with other data acquisition technologies, the powerful simultaneous localization and mapping (SLAM) algorithm can accurately capture the entire building, including the exterior wall and surrounding environment, and can reliably address all problems from complex indoor spaces to outdoor environments. A wearable mobile scanning system can realize 360° high-detail dynamic reality capture, real-time scanning feedback, and detection and removal of dynamic objects in complex sites, thereby reducing the workload of manual data processing. Therefore, a wearable mobile scanning system can completely acquire fine point cloud data inside and outside historical buildings.

Obtaining the point cloud of the target building based on digital means and technology and realizing its high-precision three-dimensional reconstruction is one of the basic processes of historical building protection and restoration. HBIM technology has been most widely used in conservation studies of historic buildings, especially in combination with 3D laser scanning technology for model reconstruction, structural analysis, and data recording and archiving. For example, Banfi explored a new type of interaction between users and virtual environments and performed digital modeling based on the scan-to-HBIM-to-VR specification to improve the quality and use of HBIM in virtual reality applications [17]. Youn et al. scanned a demolished individual wooden structure in 3D and compared it with the scanned data of the whole building, and, based on the criteria of fitting actual building variables, generated a model containing information about historic buildings of all periods, which can also be used as a digital twin to analyze the deformation and damage of wooden structures [18]. Bacci et al. proposed a methodology for designing

and constructing a parametric object library based on documentary and manual data on existing structures or actually collected information to perform virtual reconstruction of cultural heritage at different scales [19]. Cheng et al. created a model of a traditional wooden structure in Taiwan in Revit using 3D scan data and repair data of the building, and obtained flexibility values for various shape modifications by rendering each member of the bracket assembly as a family component [20]. Given the differences in structural deformation, degree of damage, and complexity of historic buildings, it is particularly important to ensure that the accuracy of the digitized 3D models is within reasonable limits. For example, Z et al. used an ellipse fitting algorithm to calculate the center position of the column based on the existing restoration records to obtain the column inclination and inclination direction [21]. Nieto-Julián et al. compared the theoretical HBIM generated from the literature data with the HBIM reconstructed from TLS data to quantitatively analyze the structural differences and deformations of historical buildings [22]. Antón et al. used a three-stage semi-automatic method to analyze the deformation automatically generated by meshing and point cloud data, and used different commercial software to evaluate the accuracy of historical building information models [23]. The results of surveying and mapping accuracy show that, compared with the traditional spatial structure component dimensional accuracy and structural performance evaluation methods, which mainly rely on manual evaluation and one-dimensional approximate linear measurement [24,25], it is feasible to use three-dimensional laser scanning technology to evaluate the quality of spatial structure components [26]. Most of the above studies have focused on how to improve the quality and efficiency of constructing 3D models of historic buildings by improving standards and precision analysis methods. However, the models constructed using HBIM technology can be further transformed into structural analysis models to evaluate the stability and durability of historic buildings. For example, Zouaoui et al. combined 3D laser scanning technology and HBIM technology to create two numerical models: a three-dimensional model for architectural archaeology and a computational model for structural analysis [27]. Chen et al. proposed a method for evaluating the seismic capacity of architectural heritage based on high-precision 3D data, which pointed out that modeling accuracy and parameter selection are critical to simulation accuracy [28]. Antón et al. pointed out based on a case study of a cathedral that accurate heritage modeling is needed to support structural safety analysis, rather than overly simplified methods [29]. Massafra et al. performed parametric 3D modeling and developed a scientific, consistent, repeatable, and standardized monitoring protocol based on the core process of HBIM to protect architectural heritage by periodically monitoring the status of each truss [30]. In addition, it is also necessary to study how to integrate HBIM technology with the archiving and filing of historic building information in order to document the current status and changes of historic buildings. Cheng developed a complete process for digital recording and archiving of cultural heritage based on laser scanning technology [31]. Bruno et al. developed a HBIM method to support the documentation, management, and conservation planning of historic buildings [32].

In this study, the wearable mobile scanning system is used in the point cloud data acquisition of traditional buildings in eastern Fujian, aiming to overcome the heavy workload of traditional data acquisition technology and the problem of scanning field of view limitations and mutual occlusion in complex areas using technologies such as terrestrial laser scanning and UAV photogrammetry. Based on the acquired point cloud, referring to the model reconstruction process in HBIM conceptualization work, the reconstruction process of old houses in the Republic of China with the characteristics of traditional architecture in eastern Fujian is refined. Modern modeling technology is used to realize the acquisition of two-dimensional drawing surveying and mapping data and three-dimensional model data of traditional residential buildings in eastern Fujian. The accuracy of the acquired three-dimensional model is evaluated to verify the feasibility of the method used in this paper.

## 2. Methods

The 3D reconstruction method of historical buildings based on NavVis VLX2 (a wearable mobile scanning system) has three parts: data acquisition and processing, 2D drawing of historical buildings, and 3D reconstruction. The technical process is shown in Figure 1.

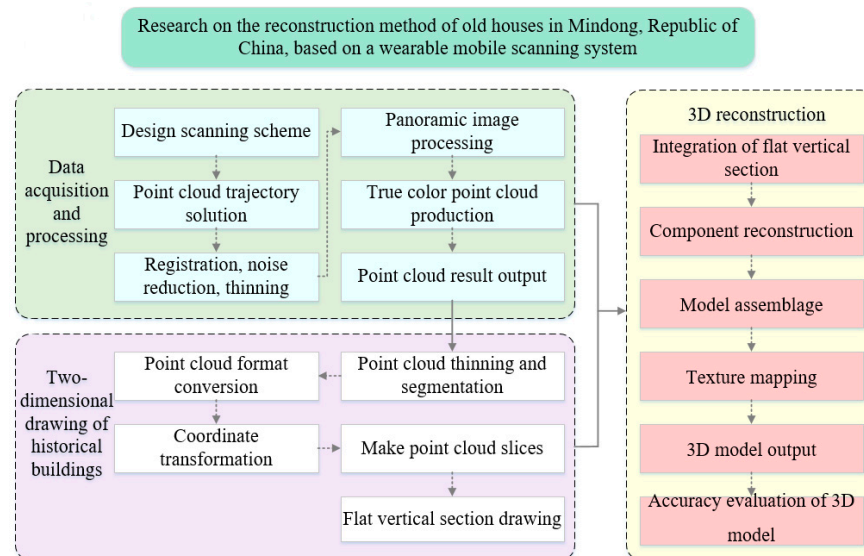


**Figure 1.** Technique flow chart.

- (1) Data acquisition and processing: (1) Historical buildings have a large number of components and a large amount of structural size information. To obtain a complete 3D point cloud, before data acquisition, field reconnaissance should be performed, and scanning path planning should be planned according to the characteristics of building layout and structural distribution to ensure the accuracy and integrity of data acquisition. (2) After the acquisition of point cloud and image data is complete, the trajectory of the acquisition can be calculated accurately by trajectory calculation so that the SLAM algorithm can be used to correct the point cloud in space and eliminate the motion distortion and deformation error. (3) Point clouds are registered at different positions, unified to the same coordinate system. (4) The point cloud is denoised and thinned to remove noise points and redundant points to improve data quality. (5) The acquired panoramic image is corrected and fused with the processed point cloud to generate a true color point cloud. The final point cloud is exported according to the modeling requirements.
- (2) Two-dimensional drawing of historical buildings: (1) Thinning and segmenting the resulting point cloud to solve the problem of point cloud format conversion failure caused by excessive point cloud data. (2) Format conversion of the processed point cloud is done to ensure its compatibility with and import into the drawing software. (3) When a single surface is drawn in the plane, elevation, and section, to reduce the accuracy problem caused by the projection angle of the point cloud in CAD2018 software, coordinate transformation of the point cloud is necessary to ensure that it is displayed in the drawing software. (4) According to the principle of simple mapping and drawing, the complete slice data of different drawing surfaces are obtained by changing the position and thickness of slices to ensure the complete presentation of each surface of the building. (5) Reference mapping standards are combined with point cloud slices and image data to complete the 2D rendering.
- (3) 3D reconstruction: (1) The plane, facade, and profile of the building are carefully integrated to ensure that they are successfully imported into the modeling software. According to the characteristics of historical building components, the layers are created and the components are created as groups and inserted into the correspond-

ing layers according to the categories so that the components in each layer form an independent whole, which is easy to modify and edit. (2) Using the hierarchical modeling strategy, the initial stage focuses on the reconstruction of each layer component; then, through precise connection, ingenious combination, and detailed deepening processing, the panorama of the 3D model is gradually constructed, which ensures that the modeling process is systematic and efficient. (3) Texture mapping of the model is completed by correcting the mapping photographs, seamless splicing, and tone adjustment to ensure the realism of the 3D model and reproduce the original style of the historical building. (4) Based on the 3D model, components with a uniform distribution and obvious characteristics of historical buildings are selected. By comparing the fitting results of the point cloud data with the actual size of the 3D model, the accuracy of the model is evaluated to ensure the accuracy and reliability of the 3D reconstruction work.

### 3. Experiments

#### 3.1. Research Object

Mindong is a geographical and cultural area in northeastern Fujian Province, China. It is the largest settlement of She nationality in China. It has profound traditional characteristics of Fujian, was influenced by Wuyue and Waifan cultures, and has unique and rich forms of expression. Its architecture combines the characteristics of architectural art in the Song, Ming, and Qing Dynasties and has great research value in the history of architecture. The old house of the Republic of China, located at No. 26 Houzhang Road, Fengshan Town, is a typical wooden-framed courtyard-style building. It belongs to the quadrangle courtyard in shape. It is the most typical of medium-sized houses in the traditional houses of eastern Fujian. Based on the continuation of the regular northern courtyard, combined with the requirements of the summer climate and mountainous terrain in eastern Fujian, the courtyard in eastern Fujian has developed from a single layer to multiple layers, emphasizing the central position of the hall, with more mezzanine floors, surrounded by a connecting corridor (through the corridor), which is more square and regular, with a stronger sense of spatial sequence. In addition, the old house of the Republic of China is composed of a main house and a ring corridor. The ring corridor and the building form a contrasting effect of size, height, virtual and real, and light and shade and produce a feeling that the actual space is expanded.

#### 3.2. Point Cloud Data Acquisition and Processing

##### 3.2.1. Data Acquisition

A NavVis VLX2 scanning system was used for data acquisition. The scanner is shown in Figure 2, and its main technical parameters are listed in Table 1.

**Table 1.** Main technical parameters of NavVis VLX2 scanning system.

Category	Parameter
Number of laser scanners	2 × 16 layers.
Wave length	903 nm
Range	100 m
Points per second	2 × 600,000
Point cloud accuracy	6 mm
Number of cameras	4
Picture resolution	4 × 20 million pixels
Focus	Fixed type
Shot	Fisheye, 3.3 mm, aperture f/2.4
Visual field	Horizontal 360 degrees, vertical 360 degrees
Resolution ratio	1080 × 1920

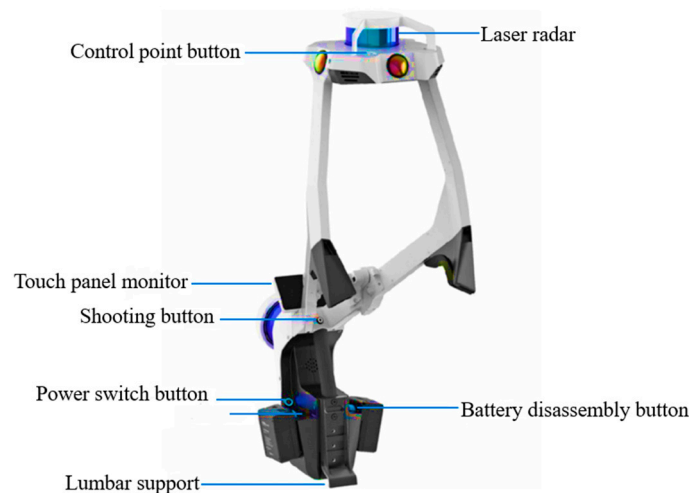


**Figure 2.** Wearable mobile laser scanner.

(1) Site survey

- (1) Understanding the natural, cultural, and traffic conditions of the working area.
- (2) Checking the authenticity and applicability of the existing data.
- (3) In the process of reconnaissance, opening the door of the building to ensure that all areas remain accessible.
- (4) Scan path planning according to the situation of the survey area.

(2) Scanning path planning.

A reasonable scanning path is essential for effective operation of the SLAM algorithm of a wearable scanning system. Therefore, the scanning path must be planned before the scanning begins. The scanning path planning process should satisfy the following criteria.

(1) The scanning range must be determined, and the scanning time must be estimated. To ensure scanning quality and accuracy, the scanning time should be controlled within 40 min. Buildings that cannot be scanned within 40 min must be scanned in blocks while ensuring sufficient overlap for subsequent model splicing.

(2) The scanning path should avoid long-distance single extensions and form multiple closed paths as much as possible to ensure intersection with the previous route and ensure the effectiveness of the SLAM algorithm.

(3) Special attention should be paid to places with lower altitudes to avoid instrument damage or inertial navigation failure caused by collision, which makes the collected data unusable.

(3) Data acquisition and panoramic photography

(1) The acquisition resolution is selected according to the planned path. When the scanning time is more than 40 min, the point cloud data are collected in turn according to the block area. The degree of overlap of the effective point cloud between the adjacent scanning areas is not less than 30%, and the overlap rate of the complex area is not less than 15%.

(2) Using a touch display screen to pay attention to the sketch map of the scanning results, the overlap of the parts should be checked, and if there is a large degree of deviation or a significant abnormality in the elevation, the scanning should be repeated.

(3) During the scanning process, 360° panoramic photography is a prerequisite for obtaining a true color point cloud model. Five meters is set as the photograph interval, and the number of shots is increased when there are more compartments or corners.

### 3.2.2. Data Processing

The acquired original scanning data were uploaded to the supporting software SiteMaker, and the point cloud data were preprocessed after engineering creation, point

density setting, and data format setting. The processing contents included trajectory calculation, point cloud registration, noise reduction and thinning, image processing, true color point cloud production, and result output. The specific process is as follows.

- (1) Trajectory calculation: The trajectory is calculated according to the inertial measurement unit (IMU) and global navigation satellite system (GNSS) data of the backpack mobile scanning system. By fusing the IMU and GNSS data, the point cloud and motion trajectory collected by the scanner can be synchronized in time, and the point cloud can be spatially corrected according to the motion trajectory of the scanner, thereby eliminating such errors as motion distortion and deformation and obtaining a more accurate 3D point cloud.
- (2) Point cloud registration: Point clouds in different regions are matched and spliced to form a unified whole, ensuring correspondence between the real scene and the actual geographical location.
- (3) Noise reduction and thinning: The abnormal and isolated points in the point cloud that are separated from the scanning target are denoised by human–computer interaction. In addition, the high density of the point cloud can be reduced by thinning to ensure that the target feature recognition and extraction are not affected.
- (4) Panoramic image processing: The backpack mobile scanning system can simultaneously capture panoramic photographs while scanning the target point cloud. However, because of the different light conditions of the scanning path, the captured panoramic photographs have overexposed, underexposed, shadowed, and adjacent images. There are differences in color; therefore, it is necessary to adjust the color of the photograph to ensure that the image contrast is moderate and that the color is consistent.
- (5) True color point cloud production: In registration mode, the point cloud and view image are fused by controlling translation and rotation. Different regions are distinguished by color for recognition, and the degree of overlap of the different regions is verified to complete the production of a true color point cloud.
- (6) Result output: Based on the modeling requirements, a high-quality and high-precision point cloud 3D model in .las format is generated. The point cloud data processing results are shown in Figure 3.



**Figure 3.** Point cloud model.

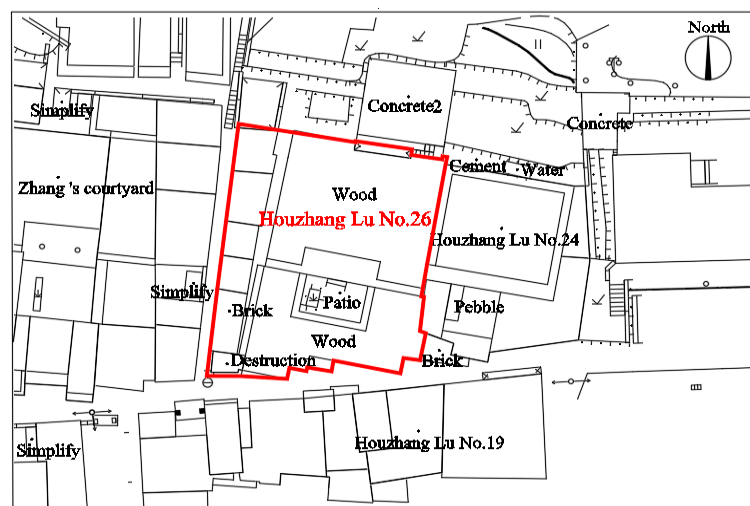
### 3.3. Two-Dimensional Rendering

Point cloud slicing is essential to the accurate drawing of flat and vertical sections of old houses in the Republic of China. Firstly, due to the huge amount of point cloud data, the point cloud format conversion failed, and point cloud thinning and segmentation work were required. This study used the non-uniform lossless thinning algorithm [33] to thin the building point cloud set, and designed a point cloud segmentation tool. The area segmentation method is used to complete the model segmentation, making the point cloud data lightweight and completing the point cloud format conversion work. Secondly, the Autodesk ReCap2016 software is used to convert the segmented point cloud into the .rcp format and import it into AutoCAD in turn. Then, according to the characteristics

of the old houses of the Republic of China and the functional requirements and details of various drawings, different scales are selected, and necessary layers are set according to the “Unified Standard of Building Construction Drawing” [34] and “Ancient Building Surveying and Mapping Specification” [35]. Finally, according to the point cloud slice, the principle of simple mapping (the drawing content only expresses the overall outline of the building and the outline of the components) is employed for drawing. When the horizontal and vertical sections are drawn, the one-to-one correspondence principle is followed—that is, after the single-view drawing is completed, the next picture is created to ensure consistency and accuracy between the plane, facade, and section. Because the collected point cloud data cannot fully reflect the overall shape of the building owing to the lack of some of the building, the existing data are used to improve the drawings. Drawing and measurement follow the same principle—that is, “from the whole to the part, first control and then detail”—to ensure that each step is based on the overall understanding of the building to achieve a refined drawing of its structure.

### 3.3.1. General Layout Drawing

In determining the measurement range, the definition of the scope of the ontology plays an important role. The topographic map is selected as the base map and superimposed to define the measurement range clearly. On this basis, the red line boundaries of historical buildings and the outlines of buildings and surrounding buildings or structures, roads, and squares are accurately drawn to fully show the spatial positioning and surrounding environment of the building. In the figure, important information is further marked, such as the name of the target building and the main building, the location of the main entrances and exits, the traffic network, the direction of the compass, and the scale, to complete the drawing of the general plan. As shown in Figure 4, the general plan accurately reflects the surrounding geographical features of historical buildings and comprehensively reflects their cultural and historical context in urban texture.



General layout 1:200

Figure 4. General layout.

### 3.3.2. Plane Drawing

In many historical buildings, columns are designed to be narrow at the top and wide at the bottom. In addition, considering that the column as a building support structure reflects the architectural characteristics and proportional relationship, a column with a diameter of approximately 1.5 m from the ground is cut to obtain the point cloud plane slice, as shown in Figure 5. Based on the point cloud slice and the range line of the historical building body provided in the general plan, the center line of the column and wall is selected as the axis to locate the overall layout of the building. Based on the actual size and current specifications,



the foundation, column foundation, wall, doors and windows, stairs, patio, etc. are drawn, and the information is marked to complete the drawing of the building plane (Figure 6).



Figure 5. Point cloud plane slice.

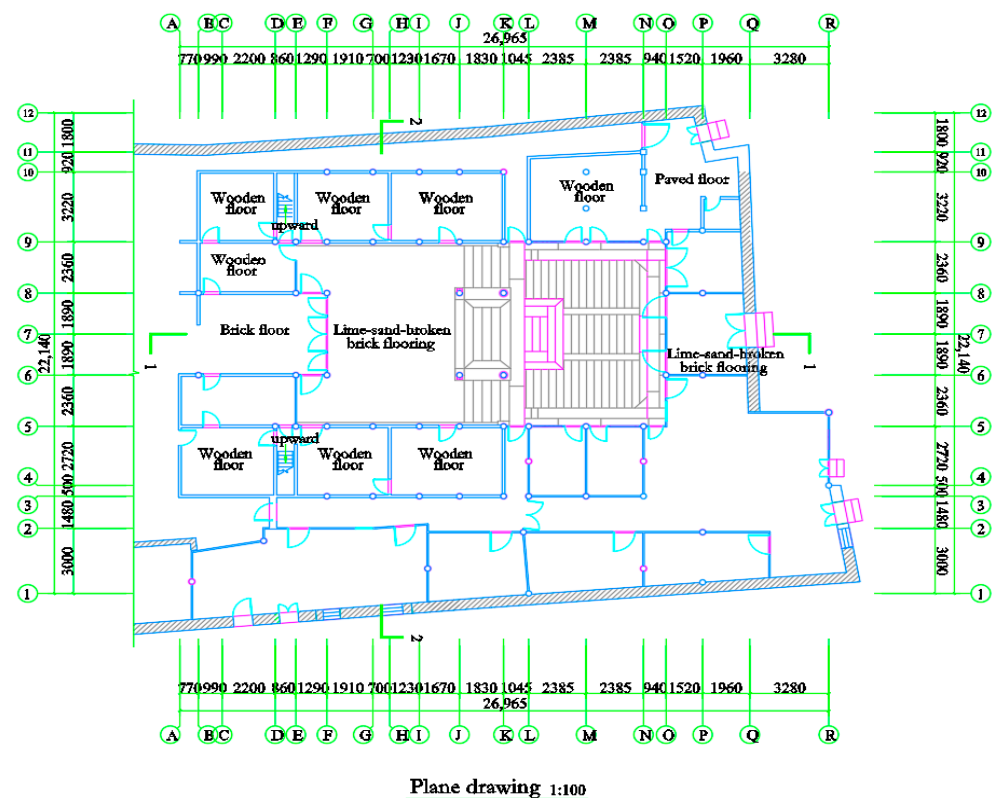


Figure 6. Plane drawing.

### 3.3.3. Facade Drawing

If the structure of the outer wall of a courtyard building is simple or severely damaged, the main house is selected as the object of the elevation drawing. The walls of the front and left facades of the old houses in the Republic of China are well preserved and reflect the needs of the houses in the eastern part of Fujian to resist wind and rain erosion and prevent moisture. The wall foundation is mostly made of granite rubble. Therefore, these two facades are selected for the elevation drawings of historical buildings. In addition, because 2D

drawings by CAD software must be done on the XOY surface, it is necessary to convert the world coordinate system to switch the facade of the point cloud 3D model to an orthographic perspective. On this basis, a point cloud slicing tool is used to eliminate the point cloud of the non-target facade to obtain clear point cloud facade slices (Figures 7 and 8). When using point cloud slices to draw the elevation diagrams, first, the positioning axis, ground line, and platform base are drawn to reflect the overall flatness of the building, and roof conditions, such as ridges, tiles, eaves, and eave boards, are drawn. Finally, the doors, windows, walls, columns, and other visual components are drawn, and the necessary size labeling is done. The front and left facades are shown in Figures 9 and 10.



Figure 7. Point cloud front facade slice.



Figure 8. Point cloud left facade slice.

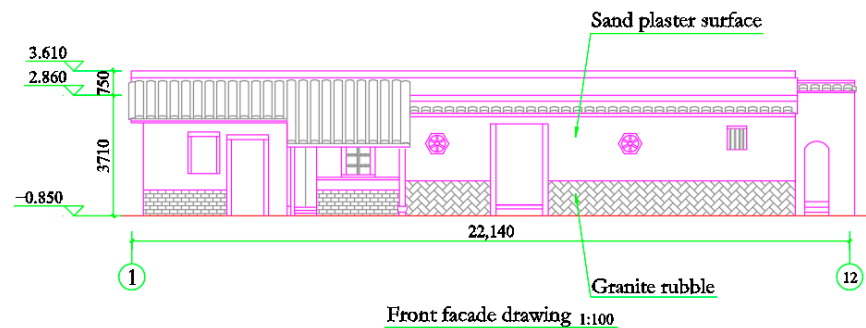


Figure 9. Front facade drawing.

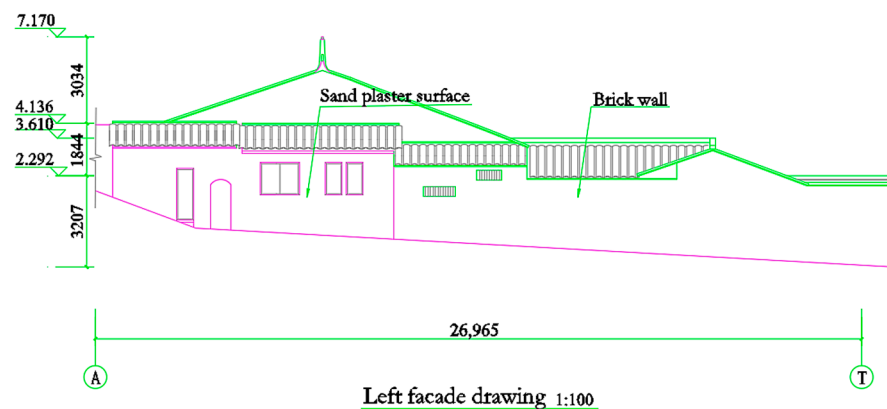


Figure 10. Left facade drawing.

### 3.3.4. Section Drawing

According to the characteristics of the overall structure of the old house of a historical building in the Republic of China, a mixed wear bucket and lifting beam structure was adopted. After satisfying the point cloud model elevation in CAD, the point cloud slicing tool is used to select the main house spine position of the point cloud model for slicing to obtain the point cloud transverse section slice (Figure 11). This is then cut along the central axis of the point cloud model, and the more complete side is selected as the vertical section slice of the point cloud, as shown in Figure 12. Using the point cloud slice as the basis for drawing the profile, the longitudinal axis in the plan is rotated and translated as the axis of the transverse profile, and the building ground line is drawn to reflect the flatness of the building. The column is drawn according to the corresponding size in the plan. The wall cut wallboard and floor are represented by section lines. The cross beam is drawn according to the overall structure and size. The typical size of the bucket arch is drawn according to the principles of French surveying and mapping. In addition, owing to the existence of multi-layer visual beam frames, it is necessary to capture accurately and completely present all building structures displayed along the cut-off line when drawing the profile. The cross section and longitudinal section are shown in Figures 13 and 14.



Figure 11. Point cloud transverse section slice.



Figure 12. Point cloud vertical section slice.

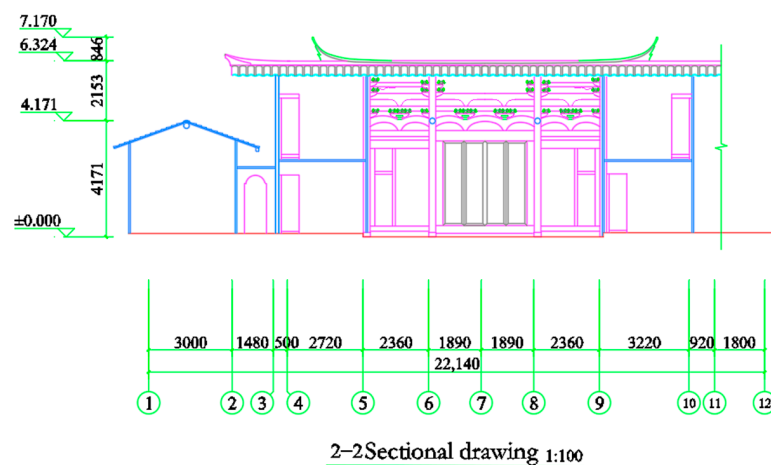
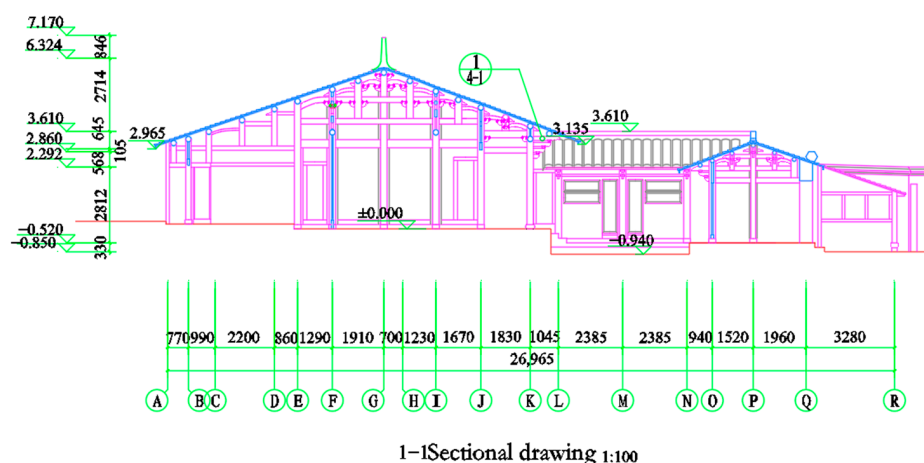


Figure 13. 2-2 sectional drawing.



**Figure 14.** 1–1 sectional drawing.

### 3.3.5. Detail Drawing

Considering the complex structures of historical buildings, a large number of drawings are typically used to show the details of buildings more clearly. This type of architectural drawing is called an “architectural detail.” Building details and plans, elevations, and sections complement each other and are mainly used for building plans, elevations, and sections that cannot be fully expressed in the local structure of the building, building details of the supplement, or description. There are many details of old houses in the Republic of China, and there are many structures, decorations, and materials that reflect historical features and local characteristics. As a load-bearing component with outstanding historical value in the old houses of the Republic of China, bucket arches are usually used to support the vault, roof, or roof truss of a building, which play roles in load bearing, earthquake resistance, and decoration. They are also a symbol of building grade, reflecting the historical development of Chinese wood-structure buildings. Therefore, a detailed drawing of the arch under the eaves of the central room of Chen Zhai, a historical building in the Republic of China, was conducted. Its size could be clearly expressed on a scale of 1: 100. The drawing process was as follows.

- (1) The redundant point cloud is removed, except for the eaves bracket, and imported into AutoCAD after format conversion.
- (2) In CAD, the 3D model of the bucket arch point cloud is processed by horizontal and vertical sectioning (the same as in Sections 3.3.3 and 3.3.4, requiring each side of the bucket arch to face up in CAD). The flat and vertical sectioning point cloud slices of the bucket arch are shown in Figure 15a,c,e.
- (3) The contour line of the bucket arch point cloud slice map is extracted, the bucket arch ratio is appropriately adjusted according to the principles of French surveying and mapping, and a three-view drawing of the bucket arch is completed in combination with the image data.
- (4) Size labeling, text labeling, image naming, and scale labeling are performed. The detailed drawing of the bucket arch under the eaves of the central room is shown in Figure 15b,d,f.

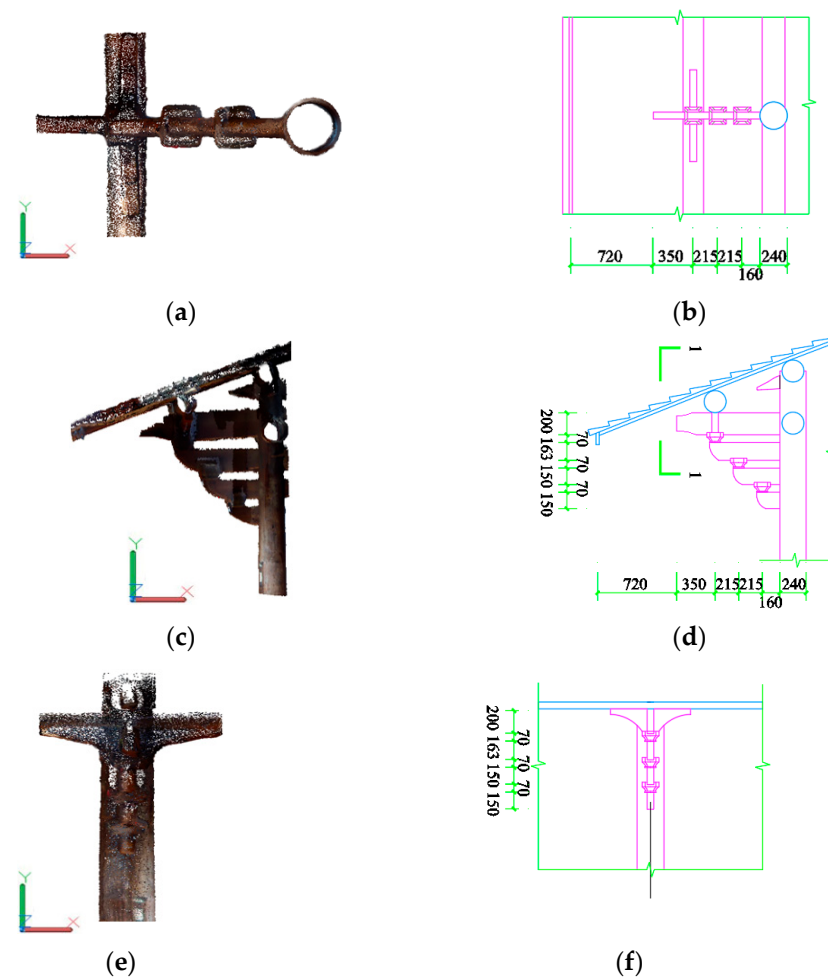


**Figure 15.** Detailed drawing of the bucket arch under the eaves of the central room. (a) Bucket arch plane slice; (b) bottom view; (c) bucket arch facade slice; (d) side elevation; (e) bucket arch section slice; (f) 1–1sectional drawing.

### 3.4. 3D Reconstruction

To realize the 3D reconstruction of an old house in the Republic of China, after simplifying the flat profile and preserving the old version, it is necessary to understand and analyze the structure and layout, details and decoration, and size and proportion of the 2D drawings. Taking the main house with the most complex structure of the old house in the Republic of China as an example, there are many components on the beam frame and many types of bucket arch. In addition, there are other components, such as foundations, walls, doors, windows, stairs, and columns. Therefore, the building can be decomposed into basic components, and a hierarchical modeling strategy can be adopted. Starting from the specific components and gradually improving the macrostructural framework, it is helpful to control the complexity of the modeling process and ensure consistency between the local and the whole. Most BIM software provides only tools for constructing rules and standardized objects, and the available free-form geometric modeling functions are limited [36]. There are difficulties in the modeling or detailed expression of complex and irregular elements of historical buildings [37,38]. Therefore, for complex historical buildings, such as old houses in the Republic of China, the flexibility and intuition of SketchUp have significant advantages. SketchUp provides powerful free-form modeling tools, which greatly reduce the high requirements for users' spatial three-dimensional sense, allow users to create adjustable component templates, easily handle irregular geometric shapes and fine details, and improve efficiency.

### 3.4.1. Component Reconstruction

A component is the basic unit of the entire building. First, the components are modeled separately and then assembled into various component models to realize the 3D reconstruction of a historical building. It has high accuracy, high flexibility, and a controllable modeling process. This ensures that the size, proportion, and geometry of each component are consistent with those of the actual building. When creating a component model of the same type in large numbers, the created single-component model can be reused, modified, adjusted, and combined according to actual needs. It can be used to understand and grasp the overall structure and details of the building better during the modeling process and obtain component models that satisfy different requirements. The modeling efficiency is improved. Therefore, the reconstruction was performed separately according to the characteristics of the components. The process for modeling the various components is as follows.

#### (1) Walls, doors, and windows

The walls, doors, and windows of historical buildings can be drawn simultaneously. First, because of the large number of walls and irregular shapes, it is necessary to use three views to adjust the size of the drawing. Second, based on the three views, the difference set function in SketchUp software is used to retain the door and window openings on the drawn wall model and combine the point cloud model and image data to complete the drawing of the door and window model. Finally, because some walls are not orthogonal, it is necessary to use a rotating tool to adjust the position of the doors and windows properly to maintain consistency with the direction of the wall. Part of the wall point cloud and 3D model comparison diagram is shown in Figure 16, and the door and window point cloud and 3D model comparison diagram is shown in Figure 17.

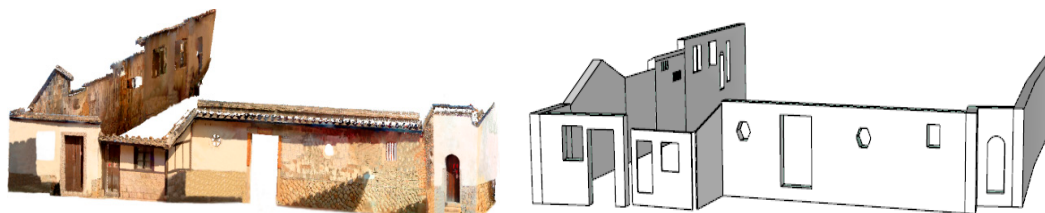


Figure 16. Wall point cloud and model comparison.

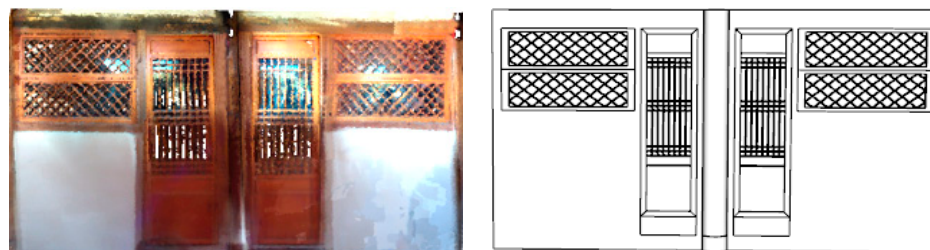


Figure 17. Door and window point cloud and model comparison.

#### (2) Columns

A column includes the column body and base, and each part must be independently constructed and finally combined into a complete unit. First, according to the plan, the cross-sectional profile of the column body and column foundation is accurately drawn. Subsequently, the specific position and elevation of the column are defined with reference to the elevation map, and the 3D shape is obtained by a stretching operation. Finally, combined with image and point cloud model data, the detailed features of the column foundation are supplemented and adjusted. A comparison between the point cloud and the 3D model of the main column is shown in Figure 18.



**Figure 18.** Column point cloud and model comparison.

### (3) Beam frame

In the 3D modeling of the beam structure, although a single structure is relatively simple, it is only necessary to draw its contour line according to the profile and perform a stretching operation to form a 3D component. However, owing to the large number of components, they are interlaced, and there is an intersection between the inner and outer beam frames when drawing the profile. Therefore, a 3D model of the point cloud must be used as a reference for detailed adjustment and optimization to ensure the integrity and accuracy of the beam frame model. Comparisons of the point cloud and 3D model of the inner and outer beam frames of the main house are shown in Figures 19 and 20.



**Figure 19.** Internal beam point cloud and model comparison.

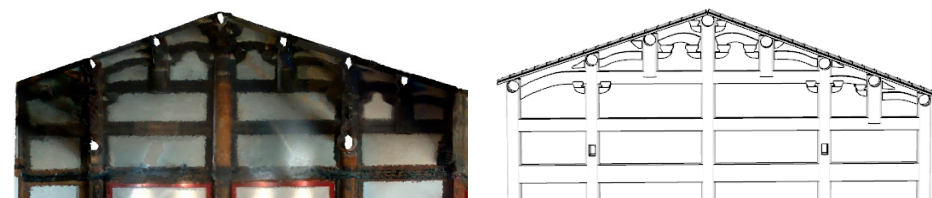


**Figure 20.** External beam point cloud and model comparison.

### (4) Bucket arch

Historical buildings in the Republic of China contain many types of bracket, but their shapes are relatively simple. They can be combined with the point cloud model and reconstructed using three views. For the arch under the eaves, the outline of the bucket and the arch can be drawn in turn using a large sample diagram and section diagram of the bucket arch, and then stretching and lofting tools can be used to construct a 3D model of the bucket arch. Because there are other bucket arches of the same type but with different sizes in the building, the size and proportion of these components must be carefully adjusted to ensure the accuracy of the overall bucket arch model. Part of the bucket arch point cloud and 3D model comparison diagram is shown in Figure 21.

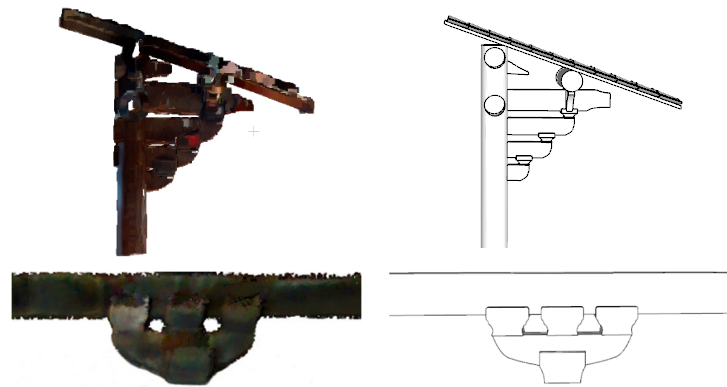


**Figure 21.** Bucket arch point cloud and model comparison.

### (5) Roof

Because the historical buildings of old houses in the Republic of China are courtyard-style buildings arranged around a patio, roof construction is more complicated. Firstly, when reconstructing the roof of the main house, the slope and ridge contour lines are drawn based on the profile and elevation map, and the model reconstruction of the roof and ridge is completed using the stretching tool. Secondly, in the digital modeling process of the corridor roof, the elevation diagram only provides partial structural information, and the slope of the roof cannot be directly inferred. Therefore, the least-squares method is used to perform plane fitting on one side of the roof and the point cloud data of the wall below to obtain the parameters of the fitting model, and then obtain the plane fitting equations of the roof and the wall. The angle between the two intersecting planes is calculated using the fitting equation, which is the slope of the roof. After determining the slope of one roof, the other two roofs can be adjusted and drawn according to the roof slope. Finally, combined with the profile, a single tile model is constructed using the arc tool, offset, push-pull, and scaling commands, and the tiles are laid on the entire roof through array replication and combined for subsequent editing and adjustment. In view of the incomplete point cloud model caused by the lack of some buildings, only the 3D model of the roof is displayed here, as shown in Figure 22.

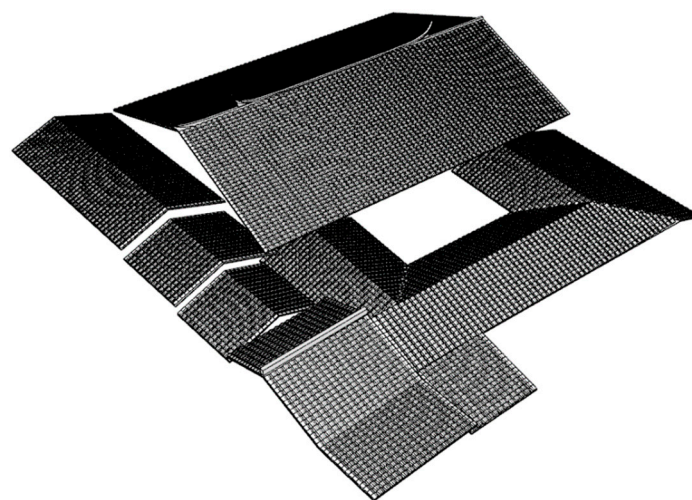


**Figure 22.** Roof model.

### 3.4.2. Model Assembly

The purpose of model assembly is to integrate the various components of a building in an orderly manner to form an independent and complete operating entity. Compared with a single component, the overall model can more fully show the appearance characteristics,



structural details, proportional relationships, and spatial layout of the building to observe and understand more intuitively the overall style of the building. In the assembly process, a 3D model of the frame is first used as the benchmark for assembly, and various parts of the building are spliced and combined by copying, translation, mirroring, and other commands. Subsequently, the details of the components are connected, adjusted, and optimized to ensure that each detail is in harmony with the overall building to complete the accurate reconstruction of the overall model (Figure 23).

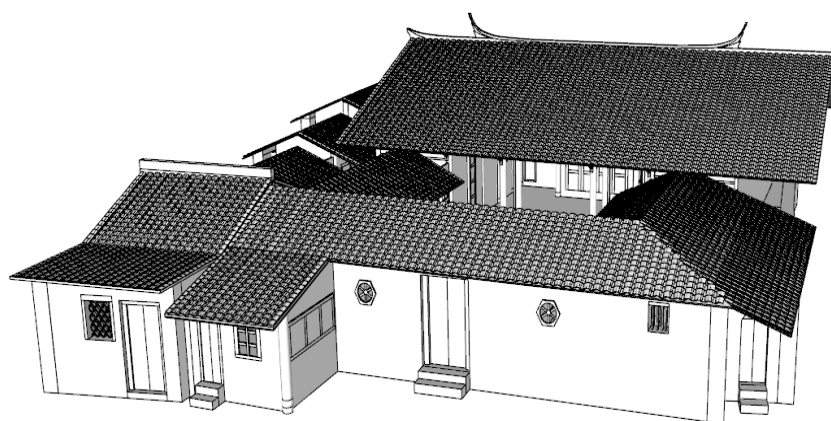


**Figure 23.** Overall model.

### 3.5. Texture Mapping

The purpose of texture mapping is to provide a higher sense of reality to the historical building model by showing the details, texture, and color of the historical building to highlight the structures and connotations of different regions. The texture data of the 3D model are derived primarily from photographs of the building. However, some photographs may be of poor quality and incomplete; therefore, it is necessary to use high-quality image materials for texture mapping. Because most of the textured photographs do not meet the requirements of texture mapping, it is necessary to pre-process them first, including correction, seamless splicing, and tone adjustment. The steps for texture mapping of historical buildings are as follows.

- (1) Correction processing: When obtaining the image information about the target, because the image is not an orthographic image, the deformation of the photograph leads to a deviation between the texture information and the actual information. It is necessary to cut, correct, and transform the picture in Photoshop to make the map more accurate and true. A comparison of before and after the correction is shown in Figure 24.

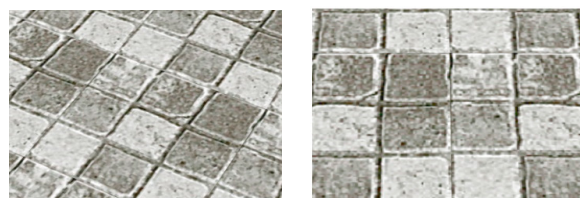


**Figure 24.** Comparison diagram before and after correction.

- (2) Stitching processing: Because the image is not folded around the relationship, there is an interval or gap between the pictures when a large number of maps are created. Therefore, the use of Photoshop's displacement and imitation seal tools can make the texture map appear more continuous and smooth, with no obvious fractures or incongruities. A comparison of pictures before and after stitching processing is shown in Figure 25.

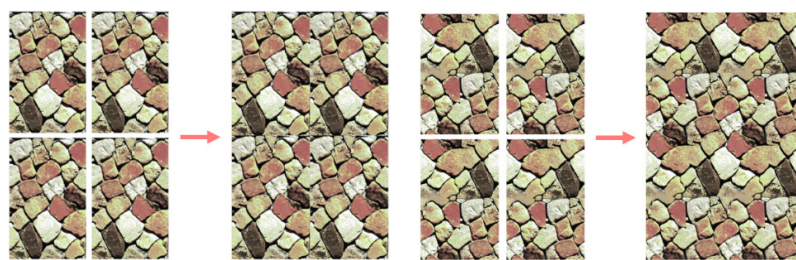


**Figure 25.** Comparison diagram before and after splicing processing.

- (3) **Tone processing:** Before the processed pictures are applied to the 3D model components of ancient buildings using the built-in material editor of the SketchUp software, it is necessary to use such tools as brightness, natural saturation, and color scale in Photoshop to adjust the picture color and enhance the sense of concavity and convexity. Second, based on the characteristics of the components, a plane map or surface map is selected. Finally, to coordinate the overall color of the model, the color of the map must be adjusted again after the map. The texture mapping effect is shown in Figure 26.

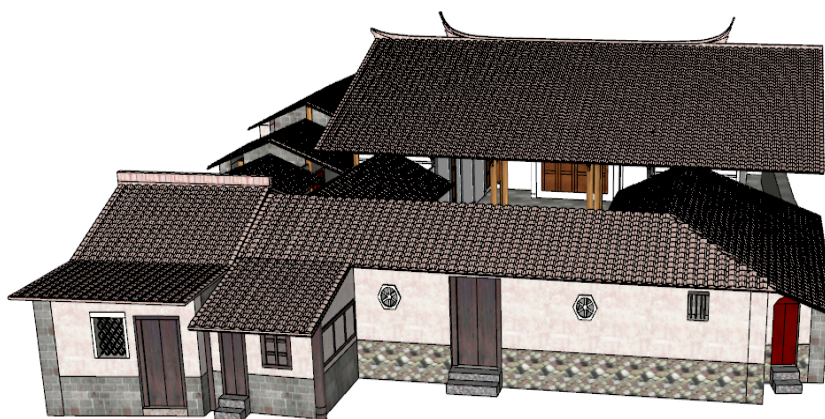


**Figure 26.** Three-dimensional model with texture mapping effect.

### 3.6. Precision Analysis

Two-dimensional graphics rendering based on point cloud slices to realize 3D model reconstruction gives each component an actual 3D model and accurate geometric size. According to the requirements for the fine measurement of historical buildings, components with a uniform distribution and obvious characteristics of historical buildings are selected. Using the least-squares method and structural geometric relationship, combined with the measured values of 3D models, the point cloud results are compared with the 3D models to evaluate and analyze the accuracy of the models. The process is as follows.

- (1) The component to be detected is divided from the point cloud model, and the selected component is then cut to obtain the point cloud data on each surface of the component.
- (2) Using the least-squares method to fit the point cloud data on each feature surface of the selected component, the parameters of the plane-fitting model can be obtained, followed by the fitting equation of each plane. The process is as follows.

For the obtained  $n$  point cloud data, the fitted plane equation is assumed to be

$$ax + by + cz + d = 0 \quad (1)$$

When the constraint condition  $a^2 + b^2 + c^2 = 1$  is satisfied, to obtain the best-fitting plane, it is necessary to minimize the square sum  $e$  of the distance from the selected feature surface point cloud data to the plane—that is, to satisfy

$$e = \sum_{i=1}^n d_i^2 \rightarrow \min \quad (2)$$

where  $d_i$  is the distance  $d_i = |ax_i + by_i + cz_i + d|$  from any point  $p_i = (x_i, y_i, z_i)$  in the point cloud data to the plane. To make  $e \rightarrow \min$ , the Lagrange multiplier method is used to solve for the extreme value and obtain the following function:

$$f = e - \lambda(a^2 + b^2 + c^2 - 1) = \sum_{i=1}^n d_i^2 - \lambda(a^2 + b^2 + c^2 - 1) \quad (3)$$

The partial derivative of  $d$  is calculated on both sides of Equation (3) when the partial derivative is zero, and one obtains

$$d = \frac{1}{n} \left( a \sum_{i=1}^n x_i + b \sum_{i=1}^n y_i + c \sum_{i=1}^n z_i \right) \quad (4)$$

If the plane centroid is  $\bar{p}(\bar{x}, \bar{y}, \bar{z})$  and  $\bar{x} = \frac{\sum_{i=1}^n x_i}{n}$ ,  $\bar{y} = \frac{\sum_{i=1}^n y_i}{n}$ ,  $\bar{z} = \frac{\sum_{i=1}^n z_i}{n}$ ,  $\Delta x_i = x_i - \bar{x}$ ,  $\Delta y_i = y_i - \bar{y}$ ,  $\Delta z_i = z_i - \bar{z}$ , then  $d_i = |a\Delta x_i + b\Delta y_i + c\Delta z_i|$ .

At this time, the partial derivatives of  $a$ ,  $b$ , and  $c$  on both sides of Equation (3) are obtained, along with the following results:

$$\left. \begin{aligned} 2 \sum_{i=1}^n (a\Delta x_i + b\Delta y_i + c\Delta z_i)\Delta x_i - 2\lambda a &= 0 \\ 2 \sum_{i=1}^n (a\Delta x_i + b\Delta y_i + c\Delta z_i)\Delta y_i - 2\lambda b &= 0 \\ 2 \sum_{i=1}^n (a\Delta x_i + b\Delta y_i + c\Delta z_i)\Delta z_i - 2\lambda c &= 0 \end{aligned} \right\} \quad (5)$$

The above equations are transformed into an eigenvalue equation, resulting in

$$Ax = \lambda x \quad (6)$$

$$\text{In the formula, } A = \begin{bmatrix} \sum_{i=1}^n \Delta x_i \Delta x_i & \sum_{i=1}^n \Delta x_i \Delta y_i & \sum_{i=1}^n \Delta x_i \Delta z_i \\ \sum_{i=1}^n \Delta x_i \Delta y_i & \sum_{i=1}^n \Delta y_i \Delta y_i & \sum_{i=1}^n \Delta y_i \Delta z_i \\ \sum_{i=1}^n \Delta x_i \Delta z_i & \sum_{i=1}^n \Delta y_i \Delta z_i & \sum_{i=1}^n \Delta z_i \Delta z_i \end{bmatrix}, x = \begin{bmatrix} a \\ b \\ c \end{bmatrix}.$$

The plane parameters  $a$ ,  $b$ , and  $c$  are then used to solve the eigenvalues and eigenvectors of the matrix. Because  $A$  is a three-order real symmetric matrix, the eigenvalue solution formula is

$$\lambda = \frac{(Ax)^T \cdot x}{x^T \cdot x}, x \neq 0 \quad (7)$$

Under the constraint condition  $a^2 + b^2 + c^2 = 1$ , one can obtain  $\lambda = \sum_{i=1}^n (a\Delta x_i + b\Delta y_i + c\Delta z_i)^2 = \sum_{i=1}^n d_i^2 = e$ . Therefore, the minimum value of  $e$  is the minimum eigenvalue of matrix  $A$ , and the corresponding eigenvectors are plane parameters  $a$ ,  $b$ , and  $c$ , which can be obtained as  $d = a\bar{x} + b\bar{y} + c\bar{z}$  by centroid.

- (3) Based on the fitting equation of the selected component feature surface, the intersection line equation between the planes can be obtained using the topological relationship between the planes. Two parallel intersection lines are selected, and one point on one of the intersection lines is selected. The vertical distance from this point to another intersection line can be calculated to obtain the size of the component feature edge.

The calculation process for a certain feature edge size of the selected component is considered as an example of a size algorithm. The calculation process of the size of a characteristic edge of a single component in the bucket arch is selected as an example of the size algorithm. The geometric relationship between the plane and the straight line in the component is shown in Figure 27.

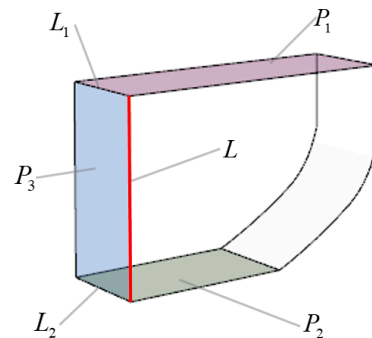


**Figure 27.** Schematic diagram of component geometric relationship.

The specific calculation process is as follows.

Using the fitting method in Equation (2), the characteristic surface  $P_1, P_2, P_3$  equations in Figure 27 can be obtained:

$$a_1x + b_1y + c_1z + d_1 = 0 \quad (8)$$

$$a_2x + b_2y + c_2z + d_2 = 0 \quad (9)$$

$$a_3x + b_3y + c_3z + d_3 = 0 \quad (10)$$

By combining Equations (8) and (10) and Equations (9) and (10), respectively, the direction vectors of the intersection  $L_1, L_2$  equation can be obtained:

$$\gamma_1 = (f_1, g_1, h_1) = \begin{vmatrix} i & j & k \\ a_1 & b_1 & c_1 \\ a_2 & b_2 & c_2 \end{vmatrix}, \gamma_2 = (f_2, g_2, h_2) = \begin{vmatrix} i & j & k \\ a_1 & b_1 & c_1 \\ a_3 & b_3 & c_3 \end{vmatrix} \quad (11)$$

Selecting each point on the intersection line  $L_1, L_2$ , respectively,  $p_1 = (x_1, y_1, z_1)$ , and  $p_2 = (x_2, y_2, z_2)$ , then the general equations of the intersection line  $L_1, L_2$  are

$$\frac{x - x_1}{f_1} = \frac{y - y_1}{g_1} = \frac{z - z_1}{h_1}, \frac{x - x_2}{f_2} = \frac{y - y_2}{g_2} = \frac{z - z_2}{h_2} \quad (12)$$

The point  $p_1 = (x_1, y_1, z_1)$  on intersection line  $L_1$  and the point  $p_2 = (x_2, y_2, z_2)$  on intersection line  $L_2$  are selected, and Equation (13) is used to calculate the distance  $d_s$  from point  $p_1 = (x_1, y_1, z_1)$  to the intersection line  $L_2$ —that is, the size of the selected feature edge  $L$ .

$$d_s = \frac{\sqrt{\left| \begin{vmatrix} y_1 - y_2 & z_1 - z_2 \\ g_2 & h_2 \end{vmatrix} + \left| \begin{vmatrix} z_1 - z_2 & x_1 - x_2 \\ h_2 & f_2 \end{vmatrix} + \left| \begin{vmatrix} x_1 - x_2 & y_1 - y_2 \\ f_2 & g_2 \end{vmatrix} \right|}}{\sqrt{f_2^2 + g_2^2 + h_2^2}} \quad (13)$$

- (4) The feature line of the bucket arch under the main eaves (the size of the marked part in the right table in Figure 28) is selected for the size calculation. There are two transparent parts in the 3D model diagram (red box selection), both of which are

inside the joint of the component. Therefore, the detailed size cannot be determined. Only the size of the external feature line is calculated and indicated, as shown in Figure 28.

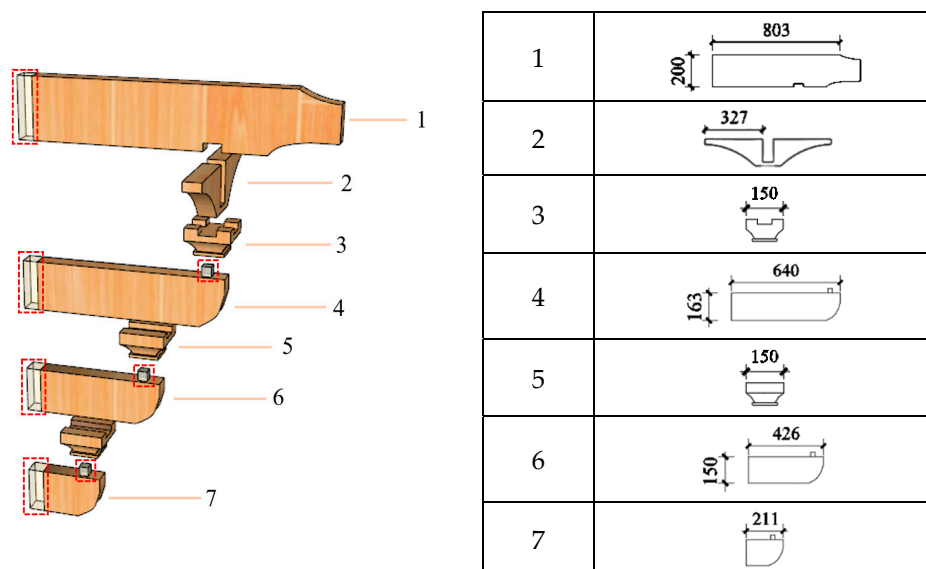


**Figure 28.** Characteristic line and size diagram (mm).

Yu used point cloud data as the true value and 3D model as the test data to compare the feature size information to verify the overall accuracy of the model. The results showed that the maximum error was 7 mm, which met the requirement of 10 mm accuracy error of the 3D model [39]. The component dimensions obtained based on the least-squares method were compared with the 3D model data. The results are shown in Table 2: the maximum error was 4.1 mm, which was also within 10 mm. This shows that the 3D reconstruction method of historical buildings proposed in the article is reasonable and meets the accuracy requirements of historical building models. The errors in the HBIM reconstruction process based on the wearable mobile scanning system mainly result from the following aspects:

- (1) Measurement equipment accuracy: The point cloud data acquisition process is affected by the accuracy of the measurement equipment, environmental conditions (light conditions and uneven reflectance), and other factors, resulting in errors in the collected point cloud data. To reduce these errors, it is necessary to calibrate the measurement equipment accurately before acquisition, select an appropriate acquisition environment, and minimize the impact of environmental factors.
- (2) Data registration errors: (1) Owing to the inconsistency of point cloud data collected at different locations or times, some information is lost, or the accuracy is lost in the process of data registration, which affects the accuracy of the final 3D model. (2) The selection and parameter setting of the registration algorithm affect the accuracy of registration. Different algorithms use different data processing methods, resulting in additional errors. (3) The errors in the early stages of data acquisition or processing are transmitted to the final 3D model through the registration process, which affects the accuracy of the model.
- (3) Model complexity: When data on complex geometric shapes or curved structures of historical buildings are collected, the occlusion problem prevents some areas from being fully captured, leading to data loss. Complex algorithms and techniques, such as surface reconstruction and feature extraction, are usually required for point cloud data processing and analysis. The implementation of these algorithms is relatively difficult, and errors can easily be introduced.
- (4) Model fitting error: When using the least-squares fitting method to fit the point cloud data, the selection of fitting parameters affects the fitting accuracy, and the fitting

function cannot fully and accurately express the characteristics of the original data, resulting in an error between the fitting results and the actual data.

- (5) Feature surface interception error: When a surface is separated from a component, different perspectives lead to different shapes and features of the observed component, which affects the accuracy and integrity of the feature surface. However, an interception thickness that is too small leads to incomplete target data, and an interception thickness that is too large contains point cloud data that do not belong to the surface.

**Table 2.** List of differences between point cloud and model size.

Fitting Sizes (mm)	Model Sizes (mm)	Error (mm)
805.2	803	2.2
201.4	200	1.4
329.2	327	2.2
147.1	150	2.9
638.2	640	1.8
160.3	163	2.7
148.1	150	1.9
423.7	426	2.3
145.9	150	4.1
213.5	211	2.5

In summary, to reduce these errors, it is necessary to control the data quality of each step strictly and ensure data accuracy to reduce the error between the actual data and the fitting results.

#### 4. Discussion

##### (1) Determination of wood structure node type

The joint connection of timber structures not only occupies a core position in the buildings of the Chinese dynasties but also plays a vital role in traditional buildings in eastern Fujian. The connection of traditional wood structure joints in eastern Fujian has technical characteristics common to traditional wood-structure buildings in other regions, which are mainly reflected in the use of mortise and tenon joints. The mortise and tenon joint is the main connection mode of traditional Chinese wood-structure buildings. The structural force system is formed by mortise–tenon joint modes, such as interpenetration, lapping, and mosaic between the wood. However, the connection of wood structure nodes in eastern Fujian is not special in the technology itself, but in its unique regional style and cultural performance. For example, in ancient houses with saddle walls, the structural characteristics of red brick and white stone and the decorative art of brackets and sparrows depend on the use of wood and the ingenious connection of wood structure nodes. The specific application of wood structure node connection technology not only ensures the structural stability of the building but also integrates the regional culture and architectural aesthetics of the eastern Fujian region in the form of expression, creating a wood structure architectural style with local characteristics.

It is precisely because of the combination of these technical details and cultural characteristics that the determination of the connection mode of the wood building structure nodes in eastern Fujian is particularly important in the 3D reconstruction of historical buildings. In the process of acquiring point cloud data of old houses in eastern Fujian by using a wearable mobile scanning system, although the current appearance of the building can be accurately recorded, it is impossible to determine the connection form of the nodes between the components of the wood structure and the specific location and size of the connection parts from the 3D scanning data. In view of this problem, especially the typical bucket arch or mortise and tenon structure in the traditional architecture of eastern Fujian, by analyzing the Caifen Zhi of Song’s “construction method” and the Doukou Zhi of Qing’s “engineering practice” the modulus system method can be used to infer

these invisible characteristics. The modular system standardizes the components of ancient Chinese buildings according to a certain scale to realize their modularization and interchangeability, providing a method for deriving other invisible feature sizes from known feature sizes. However, there are many types of mortise–tenon connection, such as straight mortise–tenon, through mortise–tenon, and dovetail mortise–tenon. Each connection mode has its unique structural characteristics and application scenarios. Therefore, it is difficult to determine what forms of mortise and tenon joints exist in historical buildings using only the point cloud obtained by the laser scanner. In order to fully understand the mortise and tenon joints of wooden structures, it is necessary to combine traditional architectural knowledge, modern detection technology, and digital modeling methods in future research.

## (2) Building structure deformation

The San Sheng Dan Ge Jia in the traditional architecture of eastern Fujian, also known as the multi-arch bent beam, is derived from the Yuanyang hand arch in the Song’s “construction method”. It is a horizontal bucket arch, and its variant structure is primarily used in the viewing frame. Its characteristics not only lie in its structural and decorative features but also in its harmonious integration with other architectural elements in the Mindong region. For example, it is combined with traditional architectural elements, such as red brick and white stone walls, hard mountain roofs, and double-warped swallowtail ridges, which together constitute the unique architectural style of eastern Fujian. In addition, the existence of the three-lift shelves reflects the continued use of the traditional wood-structure building module system in the region. Using the point cloud slicing method, a slice section of the San Sheng Dan Ge Jia that can be used for deformation analysis can be obtained. As shown in Figure 29, a deformed San Sheng Dan Ge Jia model is drawn using modeling software to ensure an accurate reproduction of its geometric status. By selecting the original undeformed state of the beam frame in the model as the reference datum line (the straight line from the starting point of the beam to the ending point) and using the built-in tape tool of SketchUp, the vertical distance of the beam frame relative to the datum line at the maximum deflection is obtained. The maximum deflection value is 76 mm. This significant downward deflection may be caused by the aging of or damage to the material used in the beam frame, resulting in a decrease in its strength and stiffness, leading to deformation under load. Considering that the position of the beam frame is a complex node where the beam, column, and bucket arch intersect in the structure, the existence of its deflection not only affects its own structural integrity but also may affect the adjacent components through the structural transfer mechanism, which in turn causes a chain reaction, resulting in a wider range of deformation and damage. Therefore, it is necessary to have a targeted monitoring and repair plan to ensure the safety and stability of the structure.

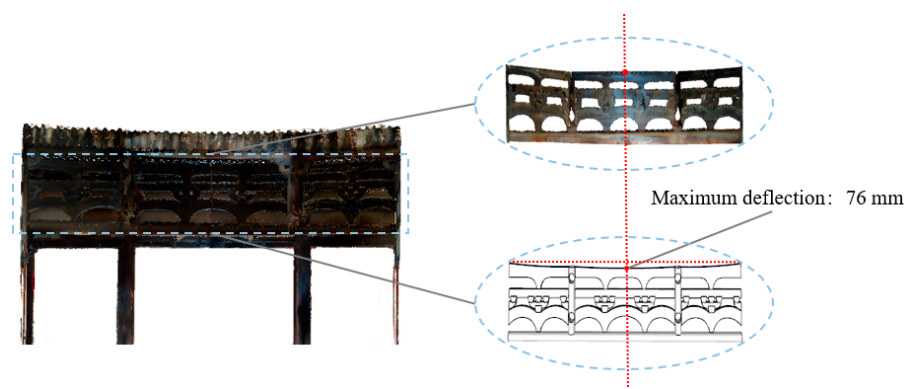


Figure 29. Deformation of beam frame and maximum deflection position diagram.

## 5. Conclusions

This article selected the old Republican houses in eastern Fujian with rich historical value as the research object, and referred to the model reconstruction process in HBIM

conceptualization work, and explored the application of the wearable mobile scanning system to carry out the research on its refined HBIM and visualization reconstruction process. The wearable mobile scanning system realizes one-button data acquisition and recording, and can conveniently carry out seamless information acquisition on the upper and lower floors, eliminating the frequent station-changing operation in the traditional surveying method, which greatly improves the convenience and continuity of data acquisition. Based on the data, the architectural heritage with traditional cultural characteristics of East Fujian can be reproduced, recorded, and preserved in the form of level and elevation profile drawings and digitized three-dimensional models to satisfy the requirements of high-precision surveying and mapping. In addition, the accuracy of the data is improved and the reconstruction process is more accurate and more precise. Based on this data, the architectural heritage with traditional cultural characteristics of East Fujian can be reproduced and preserved in the form of level and elevation profiles and digital 3D models that meet the requirements of high-precision mapping; in addition, the results of the accuracy analysis prove the rationality and effectiveness of the NavVis VLX2-CAD-SketchUp workflow in realizing high-precision mapping and model construction.

However, this article used SketchUp as a modeling software with certain limitations, such as: the inability to give historical building model attribute information, the inability to achieve data interoperability, and the need to rely on third-party plug-ins to achieve data sharing, etc., but it is consistent with this article's goal of achieving high-precision data acquisition and visualization of historical buildings. In addition, in future research, based on the high-precision data obtained by the method proposed in this article, combined with the remaining historical data and relevant historical building specifications and standards, a calculation diagram and a three-dimensional finite element calculation model of the timber frame structure that conforms to the actual situation can be established, and the corresponding internal forces, stresses, and displacements can be calculated. Then, according to the calculation results, a safety assessment of the structure can be carried out, the key factors and key parts and components that affect the structural characteristics and structural reliability can be explored, and the reasonable methods and effective measures in the construction can be analyzed, providing a theoretical basis for the protection and utilization of traditional folk houses in eastern Fujian.

Like other laser scanning technologies, the use of wearable mobile scanning systems can meet the requirements of historical building surveying and mapping, but there are still challenges in determining the form and size of the mortise and tenon joints between components. Therefore, in future research, it is possible to combine historical documents and acquired data, and the use of digital simulation technology, such as finite element analysis (FEA), to explore the simulation of the mechanical behavior of wooden structure nodes to verify the rationality of the inferred mortise and tenon joint form.

In addition, in future research on the protection of historical buildings, the structural deformation part of the point cloud model can be used to pre-identify the weak links and potential risks in the structure, so as to formulate targeted monitoring and repair plans. The use of laser scanning technology for pre-assessment can not only reduce the time wasted by blind detection, but also provide a scientific basis for repair work.

**Author Contributions:** Conceptualization, J.Y. and R.Q.; methodology, X.J.; software, W.W.; formal analysis, F.X.; investigation, W.M. and G.W.; resources, H.C.; data curation, H.C. and Y.L.; writing—original draft preparation, J.Y. and X.J.; writing—review and editing, W.M. and G.W.; visualization, X.J.; supervision, R.Q.; funding acquisition, J.Y., R.Q. and X.J. All authors have read and agreed to the published version of the manuscript.

**Funding:** The authors would like to acknowledge that this research was financially supported by the National Natural Science Foundation of China (42106180), the Science and Technology Plan for Housing Urban and Rural Construction in Anhui Province in 2022 (2022-YF169), the Provincial Natural Science Research Project of Colleges and Universities in Anhui Province (KJ2021A0612, KJ2021A1170), and the Anhui Provincial Graduate Practice Innovation Fund Project (2023CXYSJ135).



**Data Availability Statement:** The data presented in this study are conditionally available upon request from the first author.

**Conflicts of Interest:** This research was conducted in the absence of any commercial or financial relationships that could be construed as a potential conflict of interest.

## References

1. Puncello, I.; Karwacka, E. The Importance of an Integrated Historical Analysis for the Preservation of Cultural Heritage Monumental Buildings: The Case Study of Certosa Di Calci. *Int. J. Archit. Herit.* **2023**, *17*, 1542–1570. [[CrossRef](#)]
2. Dzwierzynska, J.; Prokop, A. Reconstruction of Historic Monuments—A Dual Approach. *Sustainability* **2022**, *14*, 14651. [[CrossRef](#)]
3. Charter, K. *Principles for Conservation and Restoration of Built Heritage*; Marsilio: Venice, Italy, 2000.
4. Jiang, F.Z. *A Study on the Regional Expression of Mindong Architectural Culture*; South China University of Technology: Guangzhou, China, 2015.
5. Liu, W. *A Study on the Artistic Form Features of Mindong Traditional Residential Buildings*; Fujian Agricultural and Forestry University: Fuzhou, China, 2017.
6. Owda, A.; Balsa-Barreiro, J.; Fritsch, D. Methodology for digital preservation of the cultural and patrimonial heritage: Generation of a 3D model of the Church St. Peter and Paul (Calw, Germany) by using laser scanning and digital photogrammetry. *Sens. Rev.* **2018**, *38*, 282–288. [[CrossRef](#)]
7. Yilmaz, H.; Yakar, M.; Yildiz, F. Documentation of historical caravansaries by digital close range photogrammetry. *Autom. Constr.* **2008**, *17*, 489–498. [[CrossRef](#)]
8. Wang, Q.; Tan, Y.; Mei, Z. Computational methods of acquisition and processing of 3D point cloud data for construction applications. *Arch. Comput. Methods Eng.* **2020**, *27*, 479–499. [[CrossRef](#)]
9. Alper, A. Evaluation of accuracy of dems obtained from uav-point clouds for different topographical areas. *Int. J. Eng. Geosci.* **2017**, *2*, 110–117.
10. Brumana, R.; Oreni, D.; Cuca, B.; Binda, L.; Condoleo, P.; Triggiani, M. Strategy for integrated surveying techniques finalized to interpretive models in a byzantine church, Mesopotam, Albania. *Int. J. Archit. Herit.* **2014**, *8*, 886–924. [[CrossRef](#)]
11. Şenol, H.İ.; Yunus, K. İnternet tabanlı veri kullanımıyla yerleşim alanlarının modellenmesi: Çiftlikköy Kampüsü Örneği. *Türkiye Fotogram. Derg.* **2019**, *1*, 11–16.
12. Senkal, E.; Kaplan, G.; Avdan, U. Accuracy assessment of digital surface models from unmanned aerial vehicles' imagery on archaeological sites. *Int. J. Eng. Geosci.* **2021**, *6*, 81–89. [[CrossRef](#)]
13. Yunus, K.; Şenol, H.İ.; Polat, N. Three-dimensional modeling and drawings of stone column motifs in Harran Ruins. *Mersin Photogramm. J.* **2021**, *3*, 48–52.
14. Li, Y.; Fritsch, D.; Khosravani, A. High Definition Modeling of Calw, Badstrasse and Its Google Earth' Integration. Master's Thesis, University of Stuttgart, Stuttgart, Germany, 2014.
15. Jiang, S.; Jiang, W.; Wang, L. Unmanned aerial vehicle-based photogrammetric 3d mapping: A survey of techniques, applications, and challenges. *IEEE Geosci. Remote Sens. Mag.* **2021**, *10*, 135–171. [[CrossRef](#)]
16. Ulvi, A.; Yiğit, A.Y. Comparison of the Wearable Mobile Laser Scanner (WMLS) with Other Point Cloud Data Collection Methods in Cultural Heritage: A Case Study of Diokaisareia. *ACM J. Comput. Cult. Herit.* **2022**, *15*, 1–19. [[CrossRef](#)]
17. Banfi, F. HBIM, 3D drawing and virtual reality for archaeological sites and ancient ruins. *Virtual Archaeol. Rev.* **2020**, *11*, 16–33. [[CrossRef](#)]
18. Youn, H.-C.; Yoon, J.-S.; Ryoo, S.-L. HBIM for the characteristics of Korean traditional wooden architecture: Bracket set modelling based on 3D scanning. *Buildings* **2021**, *11*, 506. [[CrossRef](#)]
19. Bacci, G.; Bertolini, F.; Bevilacqua, M.G.; Caroti, G.; Martínez-Espejo Zaragoza, I.; Martino, M.; Piemonte, A. HBIM methodologies for the architectural restoration. The case of the ex-church of San Quirico all'Olivo in Lucca, Tuscany. *Int. Arch. Photogramm. Remote Sens. Spat. Inf. Sci.* **2019**, *42*, 121–126. [[CrossRef](#)]
20. Cheng, Y.-M.; Kuo, C.-L.; Mou, C.-C. Ontology-based HBIM for historic buildings with traditional woodwork in Taiwan. *J. Civ. Eng. Manag.* **2021**, *27*, 27–44. [[CrossRef](#)]
21. Wei, Z.; Huadong, G.; Qi, L.; Tianhua, H. Fine deformation monitoring of ancient building based on terrestrial laser scanning technologies. In Proceedings of the 35th International Symposium on Remote Sensing of Environment (ISRSE35), Beijing, China, 22–26 April 2013; Volume 17, p. 012166.
22. Nieto-Julián, J.E.; Antón, D.; Moyano, J.J. Implementation and management of structural deformations into historic building information models. *Int. J. Arch. Herit.* **2019**, *14*, 1384–1397. [[CrossRef](#)]
23. Antón, D.; Medjdoub, B.; Shrahily, R.; Moyano, J. Accuracy evaluation of the semi-automatic 3D modeling for historical building information models. *Int. J. Arch. Herit.* **2018**, *12*, 790–805. [[CrossRef](#)]
24. Mosalam, K.M.; Takhirov, S.M.; Park, S. Applications of laser scanning to structures in laboratory tests and field surveys. *Struct. Control. Health Monit.* **2014**, *21*, 115–134. [[CrossRef](#)]
25. Park, H.S.; Lee, H.; Adeli, H.; Moyano, J. A new approach for health monitoring of structures: Terrestrial laser scanning. *Comput. Civ. Infrastruct. Eng.* **2007**, *22*, 19–30. [[CrossRef](#)]

26. Liu, J.; Zhang, Q.; Wu, J.; Zhao, Y. Dimensional accuracy and structural performance assessment of spatial structure components using 3D laser scanning. *Autom. Constr.* **2018**, *96*, 324–336. [[CrossRef](#)]
27. Zouaoui, M.A.; Djebri, B.; Capsoni, A. From point cloud to HBIM to FEA, the case of a vernacular architecture: Aggregate of the kasbah of algiers. *J. Comput. Cult. Herit. JOCCH* **2020**, *14*, 1–21. [[CrossRef](#)]
28. Chen, S.; Wang, S.; Li, C.; Hu, Q.; Yang, H. A seismic capacity evaluation approach for architectural heritage using finite element analysis of three-dimensional model: A case study of the limestone hall in the ming dynasty. *Remote Sens.* **2018**, *10*, 963. [[CrossRef](#)]
29. Antón, D.; Pineda, P.; Medjdoub, B.; Iranzo, A. As-built 3D heritage city modelling to support numerical structural analysis: Application to the assessment of an archaeological remain. *Remote Sens.* **2019**, *11*, 1276. [[CrossRef](#)]
30. Massafra, A.; Prati, D.; Predari, G.; Gulli, R. Wooden truss analysis, preservation strategies, and digital documentation through parametric 3D modeling and HBIM workflow. *Sustainability* **2020**, *12*, 4975. [[CrossRef](#)]
31. Cheng, H. The workflows of 3D digitizing heritage monuments, laser scanner technology. In *Laser Scanner Technology*; Intech: Rijeka, Croatia, 2012; pp. 183–198.
32. Bruno, N.; Roncella, R. HBIM for conservation: A new proposal for information modeling. *Remote Sens.* **2019**, *11*, 1751. [[CrossRef](#)]
33. Guoqiang, W.; Jiayong, Y.; Wei, M.; Hu, C.; Zongcheng, W.; Jie, X.; Xuejing, J. Construction Building Flatness Detection Method Based on 3D Laser Scanning. *Laser Optoelectron. Prog.* **2023**, *60*, 257–263.
34. *GB/T50001-2017*; Unified Standard of Building Construction Drawin. Industry Press of China: Beijing, China, 2017.
35. *CH/T6005-2018*; Specification for Surveying and Mapping of Ancient Buildings. Standards Press of China: Beijing, China, 2018.
36. Barazzetti, L.; Banfi, F.; Brumana, R.; Gusmeroli, G.; Previtali, M.; Schiantarelli, G. Cloud-to-BIM-to-FEM: Structural simulation with accurate historic BIM from laser scans. *Simul. Model. Pract. Theory* **2015**, *57*, 71–87. [[CrossRef](#)]
37. Bruno, S.; De Fino, M.; Fatiguso, F. Historic Building Information Modelling: Performance assessment for diagnosis-aided information modelling and management. *Autom. Constr.* **2018**, *86*, 256–276. [[CrossRef](#)]
38. Dore, C.; Murphy, M. Semi-automatic techniques for as-built BIM façade modeling of historic buildings. In Proceedings of the 2013 Digital Heritage International Congress (Digital Heritage), Marseille, France, 28 October–1 November 2013; IEEE: New York, NY, USA, 2013; pp. 1473–1480.
39. Yu, P.Y. Research on the Application of 3D Reconstruction and Virtual Reality of Ancient Buildings Based on Ground 3D Laser Scanning. Master's Thesis, Jiangxi University of Science and Technology, Ganzhou, China, 2019.

**Disclaimer/Publisher's Note:** The statements, opinions and data contained in all publications are solely those of the individual author(s) and contributor(s) and not of MDPI and/or the editor(s). MDPI and/or the editor(s) disclaim responsibility for any injury to people or property resulting from any ideas, methods, instructions or products referred to in the content.